Supporting Information

Lee et al. 10.1073/pnas.1802893115

SI Materials and Methods

Human and Murine Plasma. The human plasma samples were from the patient's first in-hospital blood sampling, typically within 4 h postfracture. Murine plasma was collected 3 h post femoral fracture via cardiac puncture from 12-wk-old female C57Bl6/J wild-type, *Hmgb1*$^{fl/fl}$, and *Hmgb1*$^{-/-}$ mice and from healthy unfractured controls. For the circulating levels of HMGB1, S100A8/A9, and HMGB1–CXCL12 heterocomplex over a 4-wk period, murine plasma samples were collected from 12-wk-old female C57Bl6/J wild-type mice at 1 h, 3 h, 6 h, 10 h, 5 d, 7 d, and 28 d after fracture injury. To assess the induction of inflammation-related cytokines by HMGB1, plasma samples were collected via cardiac puncture from 12-wk-old female C57Bl6/J wild-type mice at 0.5 h, 1 h, 3 h, 18 h, 48 h, and 2 wk post i.v. administration of 0.75 mg/kg of FR- or 3S-HMGB1. Samples were collected 3 h after i.v. administration of 0.75 mg/kg of DS-HMGB1 or 0.5 μg/kg of LPS. All human and murine samples were aliquoted, frozen, and stored at −80 °C before being thawed and assayed.

Mice. All animal procedures were approved by the institutional ethics committee and the United Kingdom Home Office (PLL 71/7161 and PLL 30/3330) and were performed on skeletally mature 12- to 14-wk-old female C57BL/6J (Charles River) and transgenic mice. *Hmgb1*$^{-/-}$ mice were generated by crossing *Hmgb1*$^{fl/fl}$ (Riken) with Rosa-CreER^{T2} mice (Jackson Laboratory), and at 10 wk of age administering three i.p. injections of 1.5 mg tamoxifen (Sigma) in a mixture of sunflower seed oil (Sigma) and 10% ethanol (VWR) on alternate days over a 6-d period. Mice were used 7 d after the last tamoxifen injection. *Hmgb1*$^{-/-}$ mice were obtained at the expected Mendelian ratio with no adverse phenotypic side effects, and *Hmgb1*$^{fl/fl}$ mice (not crossed with *Rosa Cre-ER*$^{T2+/+}$ mice) treated with tamoxifen were used as controls. Animals were genotyped by PCR of ear-clip DNA, with the primer sequences in Table S1, using the HotStart Mouse Genotyping Kit (Kapa Biosystems).

Fracture Model. Animals were anesthetized by aerosolized 2% isoflurane, given analgesia, and transferred to a warming pad. The right upper hind limb was shaved, and the skin was prepared with povidone iodine solution. After the skin was incised, the femur was exposed by blunt dissecting through the fascia lata between the biceps femoris and gluteus superficialis muscles. A commercial external fixator jig was fitted (RISystem), and a 0.5-mm osteotomy was created in the femoral diaphysis with a Gigli wire. The wound was closed with interrupted nonabsorbable 6/0 Prolene sutures (Ethicon). Immediately postoperatively all mice were given s.c. hydration, analgesia, and allowed to mobilize freely. Postoperative analgesia continued for 2 d. Mice were treated locally at the time of injury with an injection into the fascial pocket surrounding the osteotomy of 0.75 mg/kg FR-HMGB1 (HMGBiotech), 0.075 mg/kg, 0.75 mg/kg, or 7.5 mg/kg 3S-HMGB1 (HMGBiotech), 0.075 mg/kg CXCL12 (R&D Systems), or 50 μL PBS vehicle control; 50 mg/kg glycyrrhizin (Sigma), or 50 μL DMSO:PBS 1:1 vehicle control; 3 mg/kg AMD3100 (Abcam) or 50 μL PBS vehicle control; or 4 mg/kg rapamycin (LC Laboratories) or 50 μL DMSO:PBS (1:1 ratio) vehicle control. Glycyrrhizin was used to disrupt the formation of the HMGB1–CXCL12 heterocomplex, as it is the only known specific inhibitor for blocking the binding site of CXCL12 on HMGB1 (27, 28). Antibodies to HMGB1 do not specifically block the interaction with CXCL12 and may have other off-target effects. AMD3100 was used to disrupt the binding of CXCL12 to CXCR4, as it is a specific and clinically approved inhibitor of the CXCL12–CXCR4 interaction. It was used to determine the receptor through which the HMGB1–CXCL12 heterocomplex acted, using the rate of fracture healing as a measure of this interaction. We did not use AMD3100 or other inhibitors, such as anti-CXCL12, of the CXCL12–CXCR4 axis for cellular level characterizations of the G_{Alert} state, as this would have resulted in the activation and release of stem cells from their niche, CXCL12–CXCR4 signaling being well known for enforcing the quiescent G_0 state (31–36). For priming experiments, mice were treated systemically 2 wk before injury with an i.v. injection of 0.75 mg/kg FR-HMGB1, 0.75 mg/kg 3S-HMGB1, or 50 μL PBS vehicle control.

Cytokine Analysis. ELISAs were used to measure levels of TNF, S100A8/A9 (R&D), HMGB1 (IBL International), and the HMGB1–CXCL12 heterocomplex (R&D Systems; IBL International) in human monocyte supernatant and human and murine plasma samples. These were "sandwich" ELISAs where the antigen of interest was quantified between two layers of antibodies: the capture and the detection antibody. For S100A8/A9 and HMGB1, commercial kits were used according to the manufacturer's instructions. For HMGB1–CXCL12, we used the heterocomplex hybrid ELISA (24, 27). The reagents for the TNF and HMGB1–CXCL12 ELISA are listed in Table S2. Further immunoassays to quantify circulating levels of inflammation-related cytokines, TNF, IL-6, and IL-10, in mouse plasma following the i.v. administration of FR-, 3S-, or DS-HMGB1 or LPS were performed using commercial kits based on electrochemiluminescence (Meso Scale Discovery) per the manufacturer's instructions.

hMSC Osteogenesis Screen. hMSCs (Lonza) were maintained in DMEM (Gibco) supplemented with 10% FBS (Gibco), 1% L-glutamine (GE Healthcare), and 1% penicillin/streptomycin (GE Healthcare) in standard tissue-culture conditions (37 °C; 5% CO_2) and were used between passages 3–5. Human monocytes were isolated from human peripheral blood leukocyte cones [John Radcliffe Hospital, National Health Service (NHS) Blood and Transplant] by positive selection with CD14 MACS microbeads (Miltenyi Biotec) and an autoMACS separator (Miltenyi Biotec). To determine the direct effect of the alarmins—S100A8, S100A9 (supplied by T.V.), FR-HMGB1, DS-HMGB1 (HMGBiotech), and 3S-HMGB1—or LPS (ALEXIS Biochemicals) on hMSC osteogenesis, 10^4 hMSCs were plated in triplicate in the wells of a 96-well plate with various concentrations of alarmins or LPS in 200 μL of osteogenic medium. The latter consisted of maintenance medium supplemented with 100 nM dexamethasone (Sigma), 50 μg/mL ascorbic acid 2-phosphate (Sigma), and 10 mM β-glycerophosphate (Sigma). Treatment with 10 ng/mL oncostatin M (PeproTech) was used as a positive control. To determine the effects of alarmins on hMSC osteogenesis in the presence of monocytes or their products, monocytes were cocultured with hMSCs in a ratio of 10:1 (10^5 monocytes:10^4 hMSCs) in osteogenic medium with various concentrations of alarmins or LPS or were incubated with various concentrations of alarmins or LPS for 16 h, and the resulting supernatant was subsequently applied to hMSCs. To determine the effects of priming hMSCs with alarmins, hMSCs were plated in maintenance medium with various concentrations of alarmins; after 16 h this was changed to osteogenic medium alone. For all permutations, the respective medium was replaced at day 3, and at day 7 the medium was removed, cells were lysed in 20 μL Nonidet P-40 lysis buffer,

and ALP activity, which is a marker of osteogenic differentiation, was quantified using a commercial kit (WAKO Chemicals) per the manufacturer's instructions.

In Vivo MicroCT Setup and Analyses. In routine orthopedic practice and in clinical trials, longitudinal radiographic investigations are the most widely used tool for assessing the progression of fracture healing. Therefore, similar assessment of murine models of fracture healing would have increased translational relevance. Radiographic assessments of bone tissue are also well known to correlate highly with histological findings (47, 48) and have the added advantage of being nondestructive, thereby allowing longitudinal assessment of each animal. MicroCT imaging was performed using a high-speed rotating gantry-based system (Quantum FX; PerkinElmer) (Movie S1). Animals were anesthetized briefly with aerosolized isofluorane 2% for each 3-min scan. The X-ray source was set to a current of 200 μA, voltage of 90 kVp, and a field of view of 5 mm to encompass the two fixator pins closest to the osteotomy gap for a voxel resolution of 10 μm. After the scans, mice were revived in a heated box and were returned to their cages. Scans were analyzed using a commercially available microCT software package, Analyze12 (AnalyzeDirect), which permitted coregistration of scans acquired over a time course (Movie S2). The region of interest was defined as the bridging callus, which included only the tissue that formed in the osteotomy gap (Fig. S3*C*). Global thresholding (49) was performed to distinguish between mineralized (hard callus), poorly mineralized (soft callus), and nonmineralized (fibrous) tissue. Callus volume included the volume of both hard and soft callus. Callus BMD [previously known as "tissue mineral density" (49)] was the density of hard mineralized tissue and was calibrated by means of phantoms with known densities of calcium hydroxyapatite.

Mechanical Strength Testing. Mechanical strength testing is a well-established functional measure of callus/bone strength and fracture healing. Three-point bend testing was used, as it is a well-established, reproducible, and robust procedure for assessing the mechanical strength of the fracture callus and is superior to other techniques such as axial loading testing (50). Both hind limbs were harvested after the final microCT scan, immediately dehydrated, and fixed in 70% ethanol for at least 24 h. Before three-point bend testing (Fig. S3*F*), all soft tissues overlying the femurs and the external fixator were removed, and the clean femurs were rehydrated in PBS for 3 h at room temperature. The load cell was applied directly onto the callus, preloaded to a minimum of 0.03 N with the assistance of specimen protection, and rezeroed. Load was applied at a rate of 1 mm/min until failure, and force-extension profiles were recorded. The resulting data were analyzed using the Bluehill 3 (Instron) software package, and the maximum force before fracture (Fig. S3*G*) of the injured femur was compared with the contralateral uninjured femur.

Isolation of Stem Cells. A BD LSRFortessa X-20 and BD FACSAria III were used for flow cytometry and FACS, respectively. Subsequent data analyses were performed with FlowJo V10 software (TreeStar). mSSCs, mMuSCs, and mHSCs were defined and freshly isolated according to previously reported protocols (30, 40, 46). Bone cell suspensions were created by crushing femurs and enzymatic digestion with 800 U/mL collagenase (Worthington-Biochem). Bone marrow suspensions were created by extracting bone marrow plugs by flushing femurs with FACS buffer (Miltenyi Biotec) using a 25-gauge needle. Muscle cell suspensions were created by mincing thigh muscles and enzymatic digestion with 800 U/mL collagenase and 1 U/mL dispase (Gibco). Bone and bone marrow cell suspensions were also enriched by treatment for 5 min with red blood cell lysis buffer (Sigma). Thereafter all suspensions were strained through 70-μm and 40-μm filters (Greiner Bio-One) and stained with respective antibodies. Definitions were as follows: mSSC: $CD45^-Ter119^-Tie2^-AlphaV^+Thy^-6C3^-CD105^-CD200^+$; mMuSC: $CD31^-CD45^-Sca\text{-}1^-VCAM1^+$; mHSC: $lineage^-(CD2^-CD3^-CD4^-CD5^-CD8^-CD11a^-CD11b^-TER119^-B220^-Gr\text{-}1^-)c\text{-}Kit^+Sca\text{-}1^+CD34^-CD48^-CD150^+$. Antibodies were as follows: mSSC: CD45 (30-F11; BD), TER-119 (TER-119; BD), Tie2 (CD202b) (TEK4; BioLegend), AlphaV (CD51) (RMV-7; BioLegend), Thy1.1 (CD90.1) (OX-7; BioLegend), Thy1.2 (CD90.2) (30-H12; BioLegend), 6C3 (Ly-51) (6C3; BioLegend), CD105 (MJ7/18; BioLegend), CD200 (OX-90; BD); mMuSC, CD31 (MEC13.3; BioLegend), CD45 (30-F11; BioLegend), Sca-1 (D7; BioLegend), VCAM (CD106) (429; BioLegend); HSC CD2 (RM2-5; BioLegend), CD3 (17A2; BioLegend), CD4 (RM4-5; BioLegend), CD5 (53-7.3; BioLegend), CD8 (53-6.7; BioLegend), CD11a (M17/4; BioLegend), CD11b (M1-70; BioLegend), B220 [CD45R] (RA3-6B2; BioLegend), Gr-1 (RB6-8C5; BioLegend), TER-119 (TER-119; BioLegend), c-Kit (CD117) (2B8; BioLegend), Sca-1 (D7; BioLegend), CD34 (HM34; BioLegend), CD48 (HM48-1; BioLegend), and CD150 (TC15-12F12.2; BioLegend). Stem cells were also stained for the presence of surface CXCR4 (2B11; BD) and intracellular HMGB1 (3E8; BioLegend). $CD34^+$ hHSPCs were isolated from human peripheral blood leukocyte cones (John Radcliffe Hospital, NHS Blood and Transplant) by MACS (51) using the CD34 MicroBead Kit (Miltenyi Biotec) and an autoMACS machine.

Real-Time qPCR. Total RNA was isolated using TRl Reagent (Zymo Research) from cells from whole bone, bone marrow, and muscle cell suspensions using the Direct-zol RNA Miniprep Kit (Zymo Research) per the manufacturer's instructions. HMGB1 gene expression was determined by RT-qPCR and normalized to Gapdh. The amplifying primers were Gapdh (TaqMan, Mouse: Mm99999915_g1 Gapdh) and Hmgb1 (TaqMan, Mouse: Mm00849805_gH Hmgb1). All reactions were performed in a ViiA7 Real-Time PCR System (Applied Biosystems) using TaqMan Fast Advanced Master Mix (Applied Biosystems) according to the manufacturer's instructions.

Cell-Cycle Kinetics. To evaluate cell-cycle propensity, pulse labeling with BrdU (Abcam) was performed with animals injected i.p. with 10 mg of BrdU 10 h before cell isolation from whole femurs. Mice were treated locally at the time of fracture with 15 mg/kg FR-HMGB1, 15 mg/kg 3S-HMGB1, 15 mg/kg BMP2 (PeproTech), or 50 μL of PBS as vehicle control. To evaluate the speed of entry to the cell cycle, continuous labeling with BrdU was performed by administering 6.5 mg/mL in their drinking water with 5% sucrose for the indicated period. BrdU incorporation was quantified with the commercially available BrdU Flow Kit (BD) per the manufacturer's instructions. Following cell isolation and staining, cells were fixed and permeabilized with Cytofix/Cytoperm (BD) for 15 min at room temperature, buffered with Permeabilization Buffer Plus (BD) for 10 min at 4 °C, refixed with Cytofix/Cytoperm for 5 min at room temperature, treated with 30 μg/mL DNase (BD) for 1 h at 37 °C to expose incorporated BrdU, and stained with anti-BrdU (BD). Mice were treated systemically at the initiation of continuous BrdU administration with an i.v. injection of 15 mg/kg FR-HMGB1, 15 mg/kg 3S-HMGB1, or 100 μL PBS vehicle control. The cells from these mice were compared with cells from the fractured side of injured mice who had also been administered continuous BrdU.

Cell Migration. In vivo cell migration to the fracture site was determined by quantifying the number of $BrdU^-$ cells in fractured femurs 12 h postfracture using flow cytometry and Precision Count Beads (BioLegend). Mice were administered 10 mg of BrdU i.p. at the time of fracture and were treated locally with 0.075 mg/kg CXCL12 or 50 μL PBS vehicle. Subsequently, BrdU incorporation in the bone and bone marrow cell suspensions from

the fractured femurs was determined using the commercially available BrdU Flow Kit (BD) per the manufacturer's instructions.

In vitro migration of mSSCs was determined by placing 1,000 freshly FACS-isolated mSSCs in 6 μL of DMEM in the middle observation channel of collagen-coated μ-Slide Chemotaxis slides (Ibidi). A chemotactic gradient was established across the observation channel by pipetting 70 μL DMEM 0% FBS into the left reservoir, and 0.15 μg/mL or 1.5 μg/mL CXCL12 or 0% or 20% FBS (control) into the right reservoir. The channels and reservoirs were plugged to prevent evaporation, and cell migration was followed by time-lapse microscopy using an automated xyz motorized stage (Prior ProScan II; Prior Scientific), a climate chamber at 37 °C, 5% CO_2, with humidity (Solent Scientific), a spinning disk Nikon Eclipse TE2000-U microscope with a 10× objective, and Volocity 6.3 (PerkinElmer) recording software. Cells were monitored over a period of 22 h by capture of bright-field images every 5 min. The migration of 50 cells was analyzed using the automatic tracking function within the Imaris 6.7 (Bitplane) software and was represented using the Chemotaxis and Migration Tool 2.0 (Ibidi). Cells were excluded if the track length was less than 50 μm.

Mitochondrial DNA. DNA was extracted from 1,000 freshly FACS-isolated mSSCs, mMuSCs, and mHSCs and from 10,000 trypsinized hMSCs and 10,000 MACS-isolated human hHSPCs using the QIAamp DNA Micro Kit (Qiagen) per the manufacturer's instructions. mtDNA was quantified by RT-qPCR using primers amplifying the cytochrome B region on mtDNA (TaqMan, Mouse: Mm04225271_g1 CYTB; Human: Hs 02596867_s1 MT_CYB) relative to the β-globin region on genomic DNA (Taqman, Mouse: Mm 01611268_g1 Hbb-b1; Human: 00758889_s1 HBB). Mice were treated systemically with an i.v. injection of 0.75 mg/kg FR-HMGB1, 0.75 mg/kg 3S-HMGB1, or 100 μL of PBS vehicle control. The cells from these mice were compared with cells from the uninjured contralateral side of fractured animals. hMSCs were treated for 16 h with 10 μg/mL FR-HMGB1 in DMEM, 10 μg/mL 3S-HMGB1 in DMEM, DMEM vehicle control, or osteogenic medium supplemented with 10 μg/mL BMP2. Whole human peripheral blood leukocyte cones were treated for 2 h with 1.5 μg/mL FR-HMGB1, 1.5 μg/mL 3S-HMGB1, 10 ng/mL IFN-γ (Miltenyi Biotec), or RPMI (Lonza) vehicle control.

Cellular ATP. Cellular ATP levels of 1,000 freshly FACS-isolated mSSCs, mMuSCs, and mHSCs and of 10,000 trypsinized hMSCs and 10,000 MACS-isolated hHSPCs were quantified using the commercially available ATP Bioluminescence Assay Kit CLS II (Roche) per the manufacturer's instructions. Cells were pelleted, boiled in 100 mM Tris and 4 mM EDTA (pH 7.75) for 2 min, and were pelleted again. Luciferase reagent was added to the supernatant. This was then read on a FLUOstar Omega spectrophotometer (BMG Labtech), with the luminescence optic. Mice were treated systemically with an i.v. injection of 0.75 mg/kg FR-HMGB1, 0.75 mg/kg 3S-HMGB1, 0.075 mg/kg CXCL12, or 100 μL of PBS vehicle control. The cells from these mice were compared with cells from the uninjured contralateral side of fractured animals. hMSCs were treated for 16 h with 10 μg/mL FR-HMGB1 in DMEM, 10 μg/mL 3S-HMGB1 in DMEM, DMEM vehicle control, or osteogenic medium supplemented with 10 μg/mL BMP2. Whole human peripheral blood leukocyte cones were treated for 2 h with 1.5 μg/mL FR-HMGB1, 1.5 μg/mL 3S-HMGB1, 10 ng/mL IFN-γ (Miltenyi Biotec), or RPMI (Lonza) vehicle control.

Cell Size. Freshly FACS-isolated mSSCs, mMuSCs, and mHSCs, trypsinized hMSCs, and MACS-isolated hHSPCs were placed onto a hemocytometer and stained with 0.4% Trypan blue solution (Sigma). Bright-field images of the hemocytometer were acquired with an Olympus CKX41 microscope using a 40× objective lens. The analysis of cell diameter was performed manually using the Fiji distribution of ImageJ2 software (NIH) (52). Mice were treated systemically with an i.v. injection of 0.75 mg/kg FR-HMGB1, 0.75 mg/kg 3S-HMGB1, or 100 μL of PBS vehicle control. The cells from these mice were compared with cells from the uninjured contralateral side of fractured animals.

cMet Inhibition. Mice were treated i.p. twice a day for five consecutive days with 7.5 mg/kg of the c-Met inhibitor PHA 665752 (Selleck Chemicals) or 7.5 μL DMSO in 400 μL of PBS (vehicle control) or were treated once daily for two consecutive days with 0.5 mg/kg anti-cMet (R&D Systems) or 0.5 mg/kg goat IgG isotype control (R&D Systems) in 400 μL of PBS. Following the treatment period, mice were killed, and mMuSCs were isolated and stained for CXCR4 surface expression.

Hematological Injury Model. Animals were warmed in a heating box and were transferred to a restraining device, and a single i.v. injection of 150 mg/kg 5-FU (Sigma) was administered via the tail vein. Forty microliters of peripheral blood were collected from the tail vein with EDTA-containing Microvettes (Sarstedt) at the times indicated. Ten microliters of this sample was smeared onto slides, air-dried, and stained with Giemsa (Sigma) and May-Grünwald (RA Lamb) solutions, and neutrophils and leukocytes were counted with light microscopy using an Olympus BX51 microscope and a 40× objective lens to determine the differential neutrophil count. The remainder of the sample was treated for 5 min with red blood cell lysis buffer (Sigma) and stained with 0.4% Trypan blue solution (Sigma), and leukocytes were counted with a hemocytometer to quantify total peripheral leukocytes. Together with the differential neutrophil count as above, the total neutrophil count was also determined. Mice were treated systemically at the time of injury or 2 wk before injury with an i.v. injection of 0.75 mg/kg FR-HMGB1, 0.75 mg/kg 3S-HMGB1, or 100 μL of PBS vehicle control.

Muscle Injury Model. Animals were anesthetized by aerosolized 2% isoflurane, given analgesia, and transferred to a warming pad. The right lower hindlimb was shaved, and the skin was prepared with povidone iodine. Eighty microliters of 1.2% $BaCl_2$ (Sigma) was injected into and along the length of the tibialis anterior (TA) muscle (11). Immediately postoperatively all mice were given analgesia and allowed to mobilize freely; postoperative analgesia was given for 2 d. Mice were killed and TA muscles were extracted at the times indicated, fixed in paraformaldehyde (Santa Cruz Biotechnology) for 24 h, embedded in paraffin, sectioned, stained with H&E to identify centrally nucleated fibers, and imaged with an Olympus BX51 microscope using a 40× objective lens. The cross-sectional area of the fibers that were approximately midway along the proximal–distal axis of the TA muscle belly was manually measured using the Fiji distribution of ImageJ2 software (NIH) (52). Mice were injected i.m. at the time of injury or i.v. 2 wk before injury with 0.75 mg/kg FR-HMGB1, 0.75 mg/kg 3S-HMGB1, or 50 μL or 100 μL of PBS vehicle control.

Statistical Analysis. Statistical analyses were performed using GraphPad Prism 7 (GraphPad Software). Unless stated otherwise, significance was calculated using two-tailed unpaired Student's t tests. For microCT callus volumes, BMD, and in vivo cycling to continuous BrdU administration, significance was calculated using nonlinear curve fitting (Fig. S3 D and E) and the F-test. All results are shown as mean ± SD, except for curve fitting results, which are shown as mean ± 95% CI. Results were considered statistically significant when $P < 0.05$. Significant results were expressed using asterisks: $^{*}P < 0.05$, $^{**}P < 0.01$, $^{***}P < 0.001$, $^{****}P < 0.0001$. This convention was used throughout.

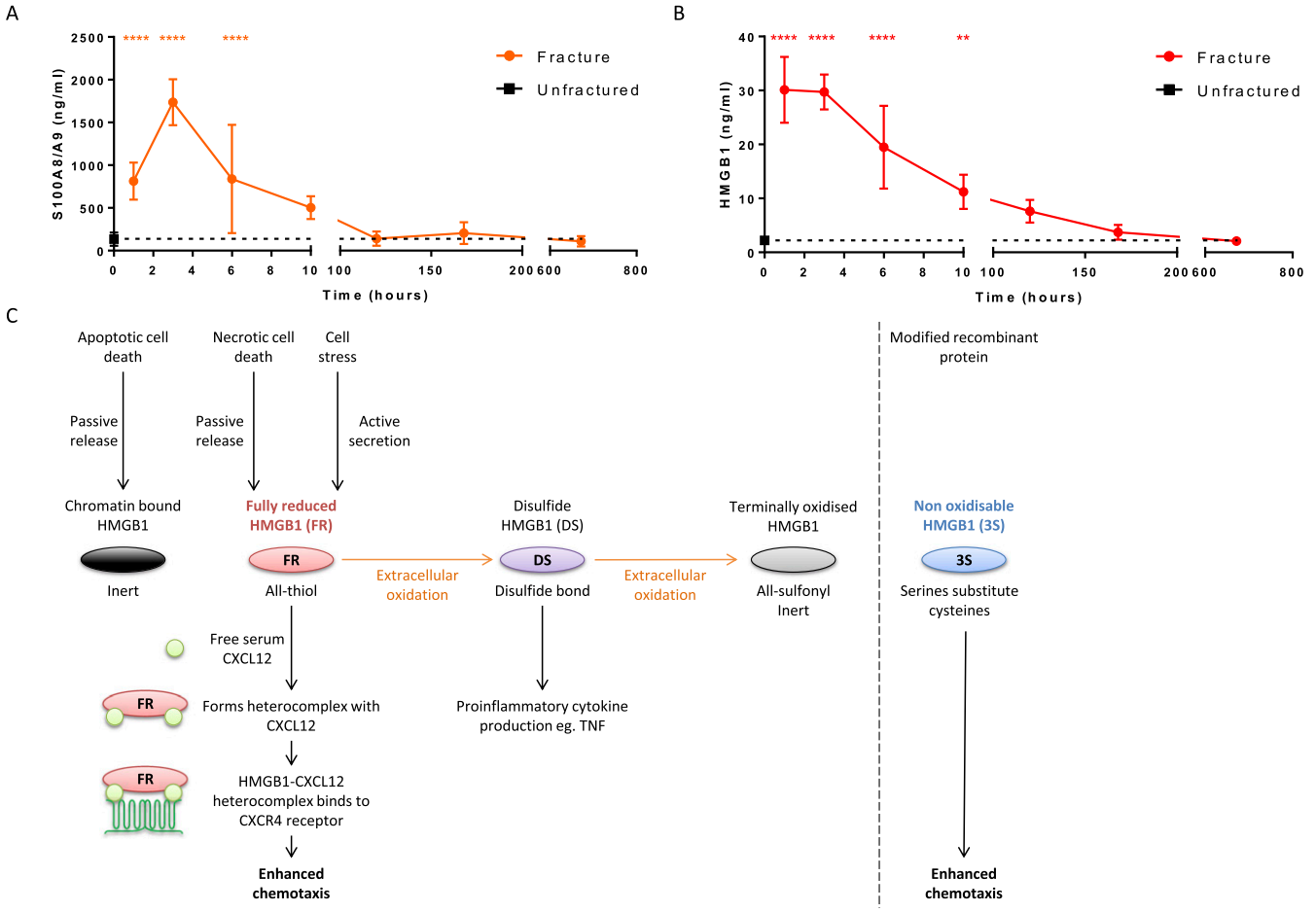

Fig. S1. Time course of alarmins postfracture and schematic of redox states and functions of HMGB1. (*A* and *B*) Circulating levels of S100A8/A9 (*A*) and HMGB1 (*B*) in plasma after femoral fracture over 28 d. Plasma samples were collected at 1 h, 3 h, 6 h, 10 h, 5 d, 7 d, and 28 d postfracture and from unfractured mice ($n = 4$ mice for each condition and time point). (*C*) HMGB1 function is dependent on the redox status. Nuclear HMGB1 is fully reduced, and in this state extracellular HMGB1 enhances the chemotactic activity of CXCL12 by forming a heterocomplex with this chemokine and binding to the receptor CXCR4. Fully reduced HMGB1 can be oxidized to the disulfide form, which is proinflammatory but has no chemotactic activity. Fully oxidized HMGB1 is inert. Replacement of cysteines at C23, C45, and C106 by serines prevents oxidation, and the molecule behaves as in the all-thiol fully reduced form. $^{**}P < 0.01$, $^{****}P < 0.0001$.

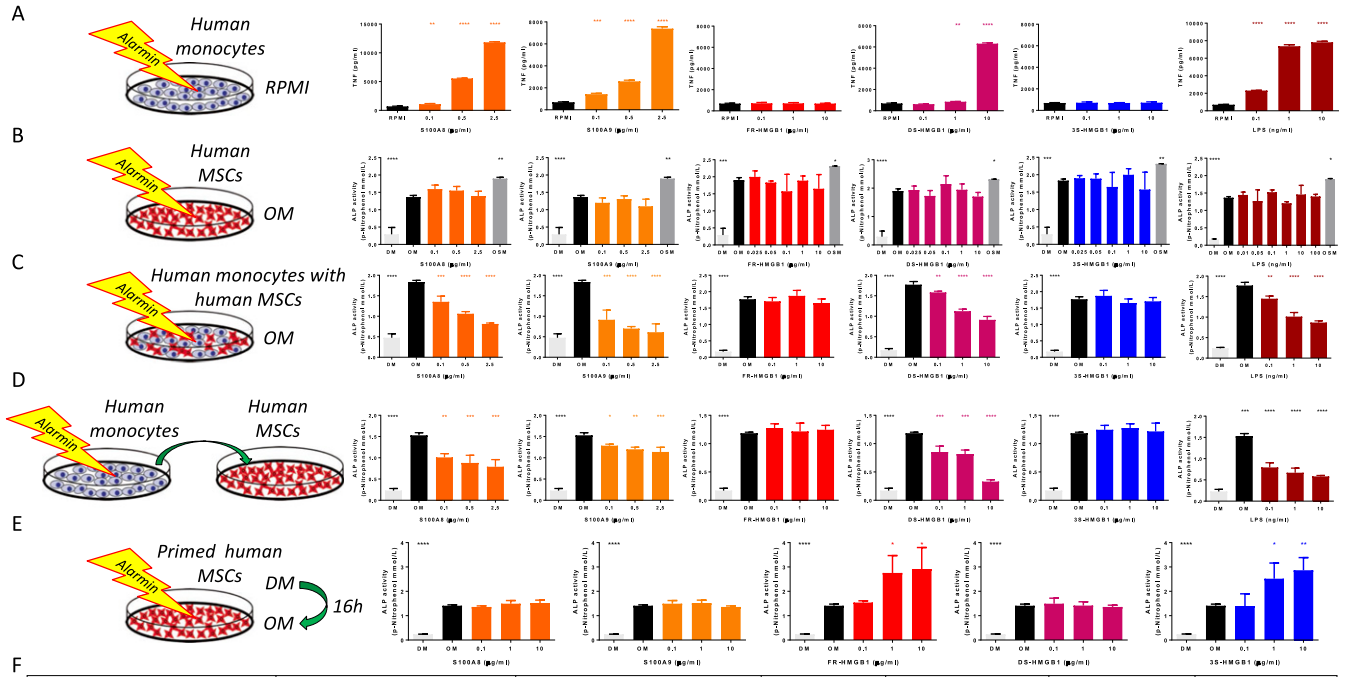

F

Early immune triggers		Elevated post-fracture in humans and mice	Inflammatory cytokine (TNF) release	Direct MSC	MSC-monocyte co-culture	Monocyte supernatant	Primed MSC
Alarmins/ DAMPs	S100A8						
	S100A9						
	FR-HMGB1						
	DS-HMGB1						
	3S-HMGB1						
PAMPs	LPS						

Fig. S2. Full human MSC and monocyte osteogenesis screen. (*A*) Only human monocytes treated with LPS, S100A8, S100A9, or DS-HMGB1 show elevated levels of TNF; significance is versus RPMI control. (*B*) No alarmin affects osteogenic differentiation when added directly to hMSCs in osteogenic medium; significance is versus osteogenic medium control. (*C* and *D*) Monocytes cocultured with hMSCs (*C*) or with supernatant from human monocytes (*D*) and treated with LPS, S100A8, S100A9, or DS-HMGB1 inhibit osteogenic differentiation of hMSCs in a dose-dependent manner; significance is versus osteogenic medium control. (*E*) Only hMSCs primed with FR- or 3S-HMGB1 show increased osteogenic differentiation; significance is versus osteogenic medium control. $n = 3$ hMSC and 3 monocyte donors for each condition for all experiments (*A*–*E*), with similar results in three independent experiments. (*F*) Heat map representation of complete in vitro osteogenesis screen of alarmins, compared with a Pathogen-associated molecular pattern molecule (PAMP, e.g., LPS), with circulating alarmins postinjury, using human plasma, hMSCs, and monocytes. Green: elevated; red: reduced; black: unchanged, gray: not applicable or not done; color brightness indicates dose trend. DM, maintenance medium; OM, osteogenic medium; OSM, oncostatin M. *$P < 0.05$, **$P < 0.01$, ***$P < 0.001$, ****$P < 0.0001$.

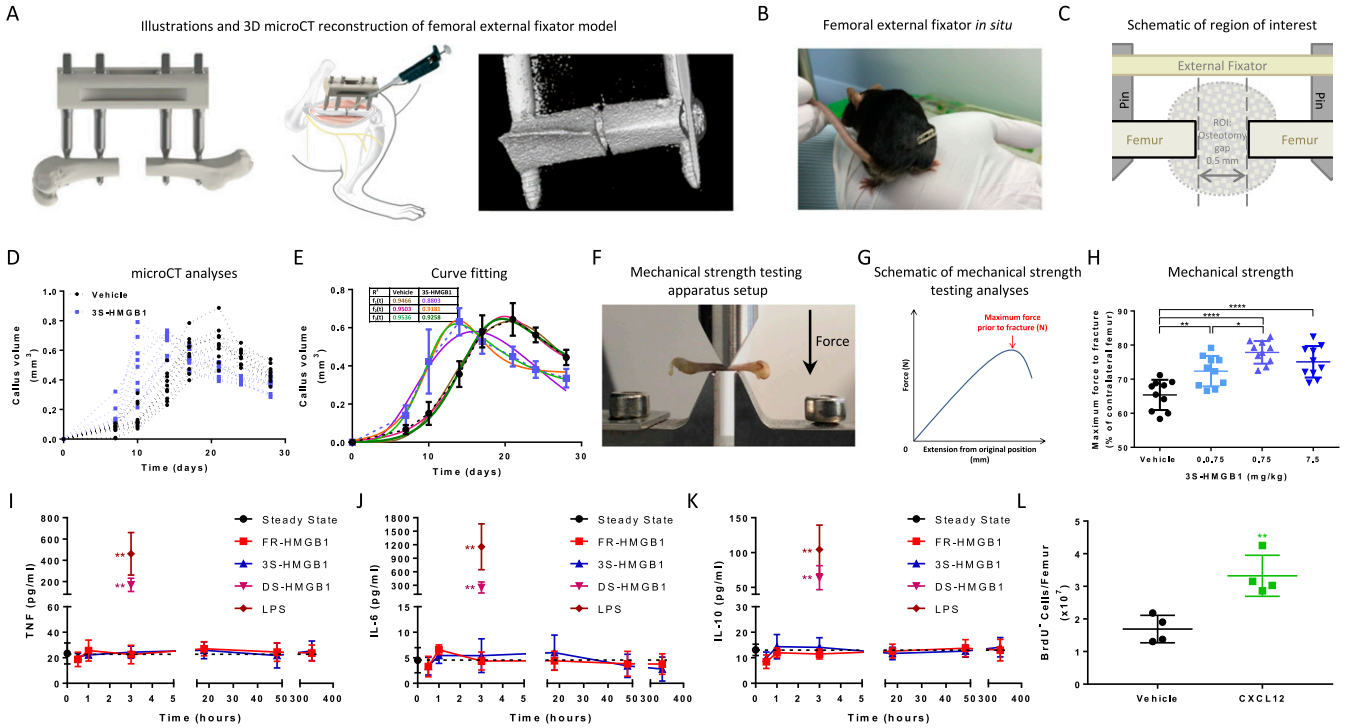

Fig. S3. Fracture healing model, analysis, and HMGB1 dose response. FR- and 3S-HMGB1 do not induce proinflammatory cytokine production in vivo, and local addition of exogenous CXCL12 increases cell migration to the fracture site. (*A*–*C*) Murine femur fracture model shown with illustrations and 3D microCT reconstruction (*A*), external fixator in situ (*B*), and schematic of the region of interest (ROI) (*C*). (*D* and *E*) Best curve fitting of callus volume data (*D*) with mathematical modeling and F-test (*E*). (*F* and *G*) Mechanical strength-testing apparatus setup (*F*) and assessment (*G*). (*H*) Mice treated locally with 3S-HMGB1 show improved fracture healing by mechanical strength testing in a dose-dependent manner, with a plateau in efficacy at 0.75 mg/kg ($n = 10$ mice for each condition). (*I*–*K*) TNF (*I*), IL-6 (*J*), and IL-10 (*K*) levels are equivalent to vehicle controls after i.v. administration of FR- or 3S-HMGB1. DS-HMGB1 and LPS were used as positive controls and resulted in elevated levels of all three cytokines, as expected. Plasma samples were collected at 0.5 h, 1 h, 3 h, 18 h, 48 h, and 2 wk ($n = 4$ mice for each condition and time point). (*L*) Local administration of CXCL12 resulted in increased migration of cells to the fracture site 12 h postinjury as shown by more noncycling ($BrdU^-$) cells per fractured femur ($n = 4$ mice for each condition). $^*P < 0.05$, $^{**}P < 0.01$, $^{****}P < 0.0001$.

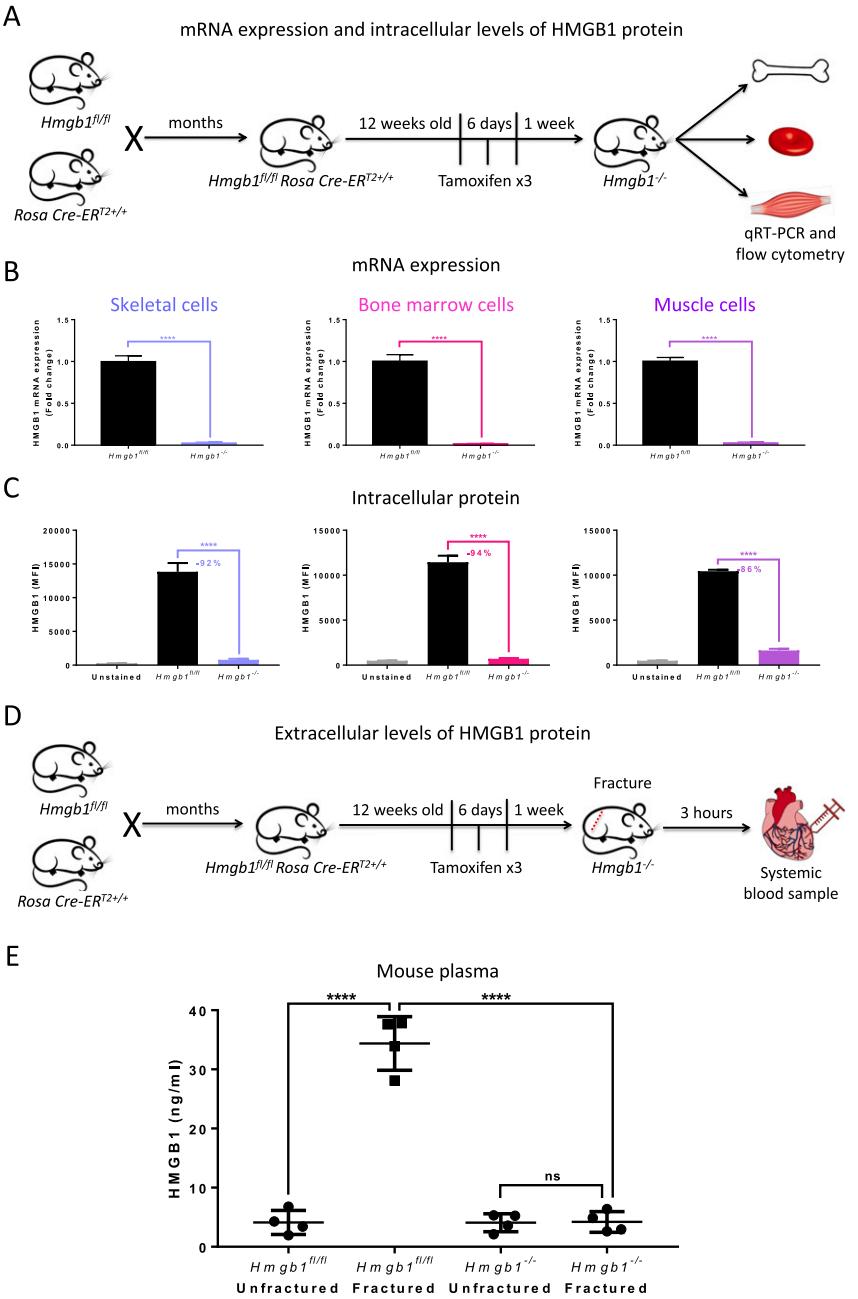

Fig. S4. Generation and validation of *Hmgb1*$^{-/-}$ mice. (*A*) Schematic of generation and timeline for tamoxifen administration and determining mRNA expression and intracellular levels of HMGB1 in *Hmgb1*$^{-/-}$ mice. (*B* and *C*) Skeletal, bone marrow, and muscle cells from *Hgmb1*$^{-/-}$ mice show markedly reduced mRNA expression of HMGB1 (*B*) and intracellular levels of HMGB1 protein (*C*) compared with *Hmgb1*$^{fl/fl}$ controls, as demonstrated by RT-qPCR and intracellular FACS staining, respectively ($n = 4$ mice for each condition). MFI, median fluorescence Intensity. (*D*) Schematic of determination of extracellular levels of HMGB1 postfracture in *Hmgb1*$^{-/-}$ mice. (*E*) Plasma levels of extracellular HMGB1 are markedly lower in *Hmgb1*$^{-/-}$ fractured mice than in *Hmgb1*$^{fl/fl}$ fractured mice and are equivalent to levels in *Hmgb1*$^{-/-}$ unfractured mice ($n = 4$ mice for each condition). ****$P < 0.0001$.

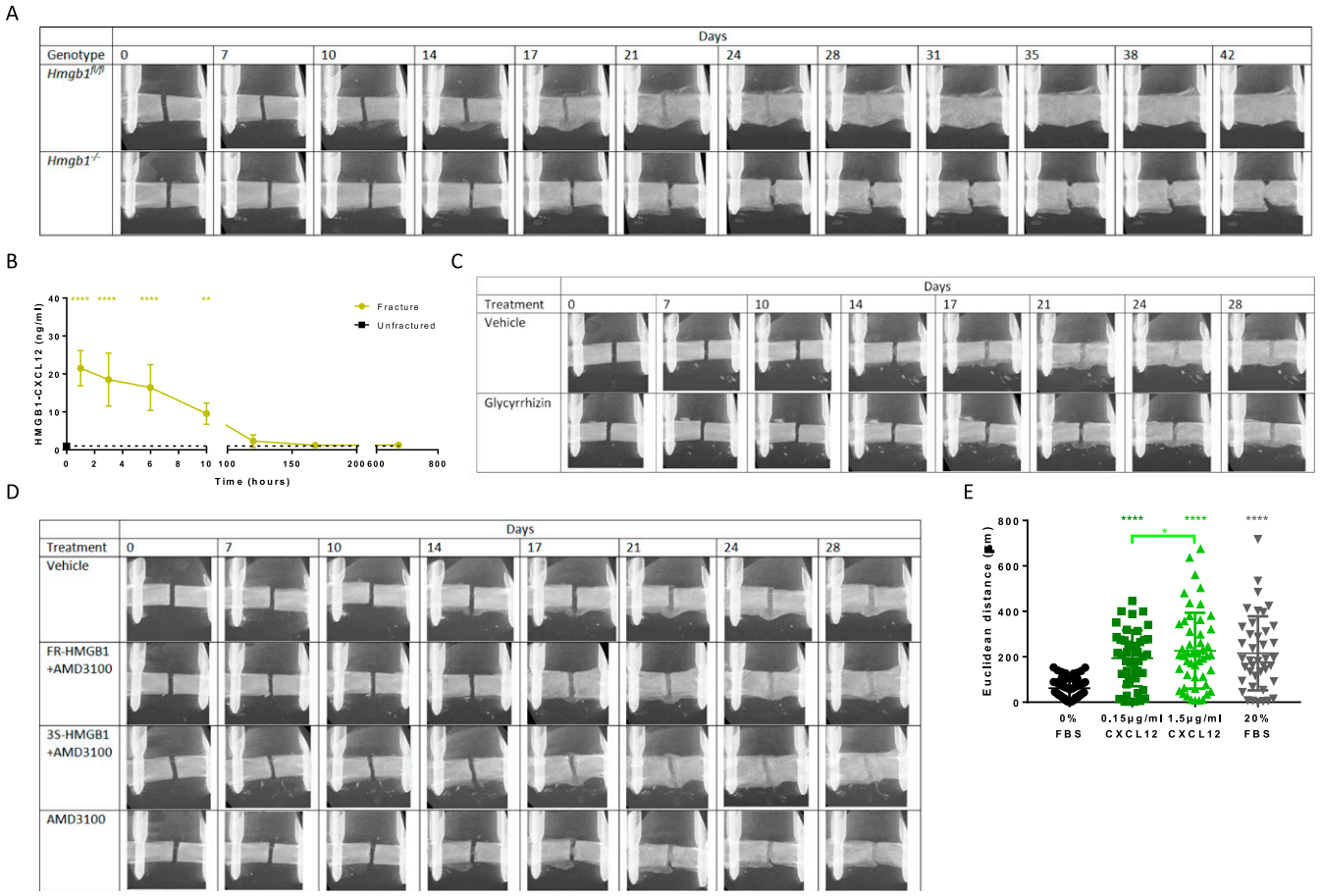

Fig. S5. In vivo microCT radiographs of genetic ablation and pharmacological inhibition of HMGB1–CXCL12–CXCR4, time course of HMGB1-CXCL12 heterocomplex postfracture, and mSSCs expressing functional CXCR4. (*A*) *Hmgb1*$^{-/-}$ mice show markedly delayed fracture healing compared with *Hmgb1*$^{fl/fl}$ controls, as shown by in vivo microCT radiographs ($n = 10$ mice for each condition). (*B*) Circulating levels of HMGB1–CXCL12 heterocomplex in plasma after femoral fracture over 28 d. Plasma samples were collected at 1 h, 3 h, 6 h, 10 h, 5 d, 7 d, and 28 d postfracture and from unfractured mice ($n = 4$ mice for each condition and time point). (*C*) Glycyrrhizin delays fracture healing compared with vehicle controls as shown by in vivo microCT radiographs ($n = 10$ mice for each condition). (*D*) AMD3100 abrogates the effects of exogenous FR- or 3S-HMGB1 as shown by in vivo microCT radiographs ($n = 10$ mice for each condition). (*E*) mSSCs migrate to CXCL12 with a dose response, as determined by time-lapse microscopy and measured by Euclidean distance ($n = 50$ cells for each condition; similar results were observed in three independent experiments). $^{**}P < 0.01$, $^{****}P < 0.0001$.

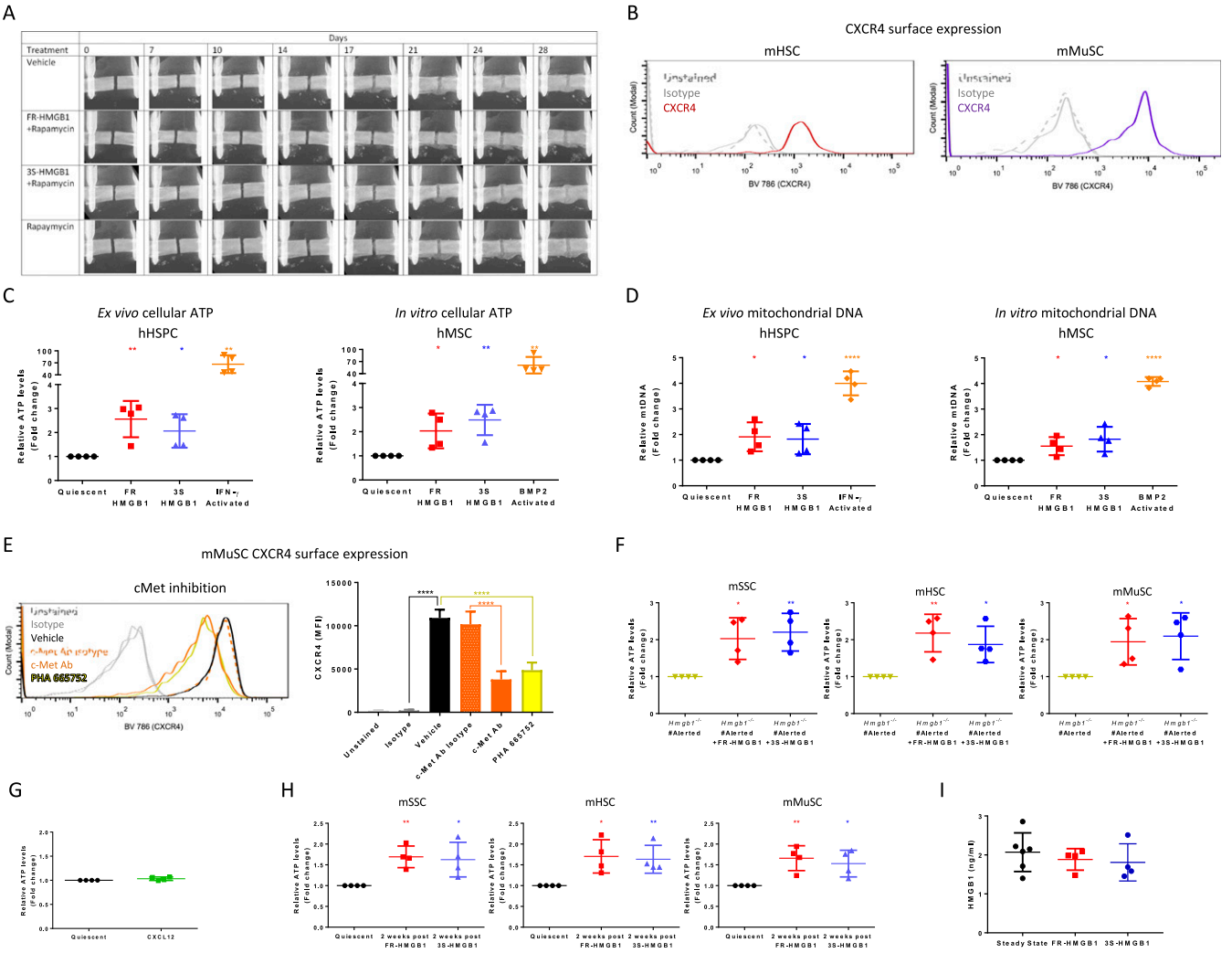

Fig. S6. HMGB1 transitions murine and human stem cells to G_{Alert}, exogenous HMGB1 rescues the ATP G_{Alert} phenotype in *Hmgb1*$^{-/-}$ mice, CXCL12 does not transition mSSCs to G_{Alert}, and stem cells remain in G_{Alert} 2 wk following i.v. HMGB1 despite circulating levels of HMGB1 returning to steady-state levels at this time. (*A*) Rapamycin abrogates the effects of exogenous FR- or 3S-HMGB1 as shown by microCT radiographs. (*B*) mHSCs and mMuSCs express CXCR4, as shown by FACS histogram plots ($n = 4$ mice for each condition, with similar results observed in three independent experiments). (*C* and *D*) hHSPCs and hMSCs treated with FR- or 3S-HMGB1 show cellular ATP levels (*C*) and mitochondrial DNA (*D*) higher than in vehicle controls but much lower than in IFN-γ or BMP2-activated cells, respectively [$n = 4$ hematopoietic stem and progenitor cell (HSPC)] donors; $n = 4$ hMSC donors, with similar results observed in three independent experiments). (*E*) mMuSCs from mice treated with a cMet inhibitor (PHA 665752) or anti-cMet, express substantially less surface CXCR4 than controls, as shown by the FACS histogram plot, and quantified by MFI ($n = 4$ mice for each condition). MFI, median fluorescence intensity. (*F*) *Hmgb1*$^{-/-}$ mice treated with FR- or 3S-HMGB1 show elevated ATP levels for mSSCs, mHSCs, and mMuSCs from contralateral limbs of fractured (#) mice ($n = 4$ mice for each condition). (*G*) Systemic administration of CXCL12 does not lead to increased ATP levels in mSSCs compared with vehicle control ($n = 4$ mice for each condition). (*H*) ATP levels of mSSCs, mHSCs, and mMuSCs remain elevated 2 wk after treatment with FR- or 3S-HMGB1 ($n = 4$ mice for each condition). (*I*) Systemic HMGB1 levels are equivalent to steady-state levels 2 wk following i.v. FR- or 3S-HMGB1 ($n = 6$ steady-state mice; $n = 4$ mice for each FR- and 3S-HMGB1 condition).*$P < 0.05$, **$P < 0.01$, ****$P < 0.0001$.

Table S1. Primers for genotyping of mice and qPCR experiments

Primer	*Hmgb1*$^{fl/fl}$	Primer	Rosa-CreER^{T2}
HMGB1 forward	TGTCATGCCACCCTGAGCAGTT	Common forward	AAGGGAGCTGCAGTGGAGTA
HMGB1 reverse	TGTGCTCCTCCCGGCAAGTT	Wild-type reverse	CCGAAAATCTGTGGGAAGTC
		Mutant reverse	CGGTTATTCAACTTGCACCA

Table S2. Reagents for TNF and HMGB1–CXCL12 hybrid ELISAs

ELISA	TNF	HMGB1–CXCL12 heterocomplex
Capture antibody	Mouse anti-human TNF (551220; BD Bioscience)	Mouse anti-human CXCL12 (DY350; R&D Systems)
Protein standard	Human TNF (210-TA; R&D Systems)	FR-HMGB1 (HM-114; HMGBiotech) and human CXCL12 (350-NS-050; R&D Systems), in a 1:2 ratio.
Detect antibody	Biotin mouse anti-human TNF (554511; BD Bioscience)	anti-HMGB1 (ST51011; IBL International)
Substrate	Streptavidin-HRP (DY 998; R&D), TMB Microwell Peroxidase Substrate Kit (507603; KPL)	Substrate A and substrate B (ST51011; IBL International)
Stop	Sulfuric acid (320501; Sigma)	Stop solution (ST51011; IBL International)
Read	Mithras Multimode Microplate Reader LB 940 (Berthold Technologies) 450 nm	Mithras Multimode Microplate Reader LB 940 (Berthold Technologies) 450 nm

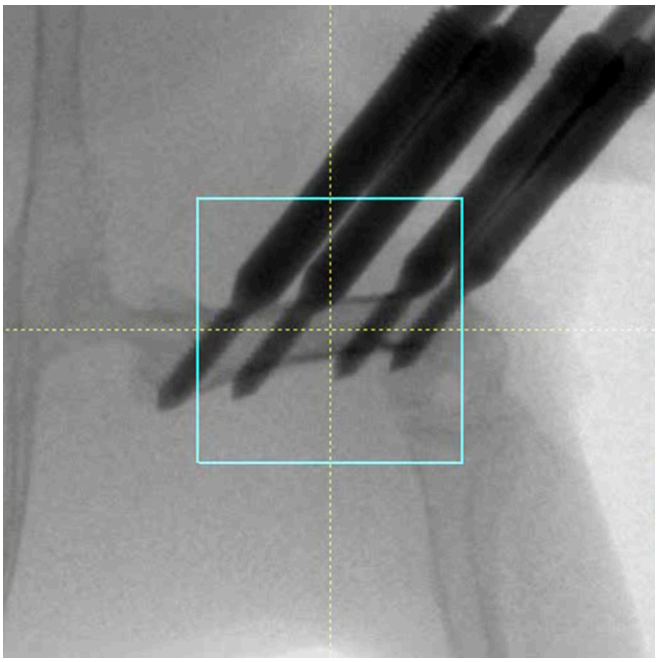

Movie S1. In vivo fluoroscopy of fracture healing. Representative in vivo fluoroscopy videos of femur at days 0, 14, and 28 postfracture.

Movie S1

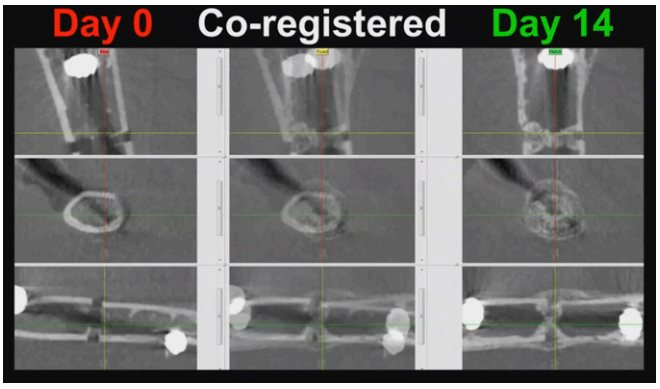

Movie S2. Coregistration of in vivo microCT images. Example of coregistration of femurs at days 0 (red) and 28 (green) postfracture.

Movie S2